

miR-451 limits CD4⁺ T cell proliferative responses to infection in mice

Lesley M. Chapman^{1,2} · Sara K. Ture¹ · David J. Field¹ · Craig N. Morrell¹

Published online: 4 April 2017

© Springer Science+Business Media New York 2017

Abstract MicroRNAs (miRNAs) are major regulators of cell responses, particularly in stressed cell states and host immune responses. Some miRNAs have a role in pathogen defense, including regulation of immune responses to *Plasmodium* parasite infection. Using a nonlethal mouse model of blood stage malaria infection, we have found that miR-451^{-/-} mice infected with *Plasmodium yoelii* XNL cleared infection at a faster rate than did wild-type (WT) mice. MiR-451^{-/-} mice had an increased leukocyte response to infection, with the protective phenotype primarily driven by CD4⁺ T cells. WT and miR-451^{-/-} CD4⁺ T cells had similar activation responses, but miR-451^{-/-} CD4⁺ cells had significantly increased proliferation, both in vitro and in vivo. Myc is a miR-451 target with a central role in cell cycle progression and cell proliferation. CD4⁺ T cells from miR-451^{-/-} mice had increased postactivation *Myc* expression. RNA-Seq analysis of CD4⁺ cells demonstrated over 5000 differentially expressed genes in miR-451^{-/-} mice postinfection, many of which are directly or indirectly *Myc* regulated. This study demonstrates that miR-451 regulates T cell proliferative responses in part via a *Myc*-dependent mechanism.

Keywords miRNA · T cell · Proliferation · myc · Malaria

Introduction

MicroRNAs (miRNAs) are 21–22 nucleotide noncoding RNA that regulate posttranscriptional gene expression by targeting the 3′ untranslated region (UTR) of mRNA transcripts. MiRNAs have an important role in diverse cell functions, including immune responses [1]. For example, miR-125b regulates CD4⁺ T cell differentiation [2], miR-223 regulates neutrophil proliferation [3], and miR-29 negatively regulates T helper type 1 (Th1) responses to *Mycobacterium tuberculosis* [4]. However, little is known about the role of miRNA in regulating host immune responses to most infections, including blood stage malaria infection. MicroRNA-451 (miR-451) is a regulator of erythrocyte development in mice [5, 6] and directly inhibits *Plasmodium falciparum* growth in vitro [7]. In mouse models of cancer, miR-451 has a role in regulating tumor cell proliferation [4, 8] and innate immune cell function [9]. MiR-451 has also been identified in CD4⁺ T cells in both healthy and disease states [10, 11], but a role for miR-451 in adaptive immunity is not known.

More than 250 million individuals are infected with the malaria causing *Plasmodium* parasite each year [12]. The immune system has a critical role in limiting malaria infection and mediating parasite clearance. In the initial stages of infection, innate immune cells, such as natural killer T cells, macrophages, and neutrophils, are responsible for direct parasite clearance. During blood stage infection, CD4⁺ T helper cells are the major mediators of the adaptive immune responses that limit infection and promote parasite clearance. Several groups have used mouse models of blood-stage malaria to demonstrate that increased CD4⁺ T cell responses correlate with reduced parasite burden [13, 14]; however, effective means to

Electronic supplementary material The online version of this article (doi:10.1007/s12026-017-8919-x) contains supplementary material, which is available to authorized users.

✉ Craig N. Morrell
Craig_Morrell@urmc.rochester.edu

¹ Aab Cardiovascular Research Institute, University of Rochester Medical Center, 601 Elmwood Avenue, Rochester, NY 14642, USA

² CTSI Translational Biomedical Science, Rochester, NY, USA

initiate and sustain acquired immune responses to infection have not been found.

We have now found that miR-451^{-/-} mice have improved clearance of nonlethal blood stage *Plasmodium* infection that is in part mediated by a protective CD4⁺ response.

Material and methods

Mouse experiments

MiR-451^{-/-} mice were created by the laboratory of Dr. Eric Olson (UT Southwestern) and are on a C57Bl6/J (B6) background. Control B6 mice were obtained from Jackson Laboratory. All mice were housed and experiments performed in accordance with University of Rochester Medical Center (URMC) Institutional Animal Care and Use Committee (IACUC) approved protocols and standards.

Mice were infected via intraperitoneal (i.p.) injection with $\sim 0.5 \times 10^7$ cryopreserved and mouse passaged *Plasmodium yoelii* 17XNL blood stage parasites (nonlethal malaria). Parasitemia was measured in 3-day intervals postinfection using Giemsa-stained blood smears.

Lymphocyte staining and flow cytometry

Spleens were collected and single cell suspensions made. For T helper cell analysis, cells were surfaced stained with anti-CD4 (RM 4–5; eBioscience), permeabilized, and intracellular stained with IFN- γ (XMG1.2; eBioscience), IL-4 (BVD6-24G2; eBioscience), ROR γ (B2D; eBioscience), CD25 (PC61.5; eBioscience), or FoxP3 (FJK-16s; eBioscience) (representative gating in Supplemental Data Fig. S1). For CD8⁺ T cells, cell surfaces were stained with anti-CD8a (53–6.7; eBioscience) and anti-CD3e (145-2C11; eBioscience). For B cells, cell surfaces were stained with anti-CD21/CD35 (8D9; eBioscience) and anti-CD19 (1D3; eBioscience). T cell activation markers CD25 (eBio3C7; eBioscience) and CD69 (H1.2F3, Biolegend) were measured using flow cytometry.

For CBC exams, ≈ 50 μ L of blood was collected into EDTA-coated tubes via retro-orbital bleed. VetScan HM5 Analyzer was used.

CD4⁺ and CD8⁺ T cell in vivo depletion

Monoclonal antibodies specific for mouse CD4⁺ T cells (GK1.5, source: Rat) were injected intravenously (0.167 mg in 100 μ L sterile PBS) on days 0, 7, and 14 and depletion confirmed by flow cytometry [15]. Monoclonal antibodies specific for mouse CD8⁺ T cells (YTS 169.4, source: Rat) were injected intravenously (0.167 mg in 100 μ L sterile PBS) on days 0, 7, and 14 and depletion confirmed by flow

cytometry. The same concentration and volume of control IgG (clone LTF-2) were used in a separate infection experiment.

Bone marrow transplantation

Femurs and tibias were collected and donor cells isolated as previously described [16]. Recipients were lethally irradiated by exposure to 830 cGy irradiation. The 1×10^6 bone marrow cells were injected into recipient mice intravenously. Sulfatrimethoprim was added to the water bottles for 4 weeks posttransplant.

Cell culture

Spleens were harvested and processed to generate a single cell suspension. Red blood cells were lysed using ACK lysis buffer (Life Technologies). CD4⁺ T cells were isolated via negative selection (EasySep; Stemcell Technologies). Purity was verified using flow cytometry. For all proliferation studies, cells were cultured in 96-well α -CD3-coated plates (1 μ g/mL; BioXCell), with 1 μ g/mL α -CD28 (PV-1; BioXCell) [17, 18]. Cell counts were measured using an automated hemocytometer (VetScan HM5). For *Myc* inhibition, cells were treated with 100 μ M 10058-F4 at D0 (Tocris). Cell death was measured via 7-AAD staining (Life Technologies) and analysis via flow cytometry with analysis using FlowJo 7.6 software.

Quantitative real-time PCR

For in vitro miR-451 measurement, purified splenic CD4⁺ T cells were stimulated for 5 days in plates coated with 1 μ g/mL α -CD3 (BioXCell) and 1 μ g/mL α -CD28 (BioXCell). Small RNAs were isolated with a miRVana microRNA Isolation Kit (Ambion) and cDNA generated using a Taqman microRNA reverse transcription kit (Applied Biosystems) according to the manufacturer's protocol. For in vitro and in vivo measurements of mRNAs, total RNA was isolated from negatively selected splenic CD4⁺ T cells using RNeasy Plus Micro Kit (Qiagen). A myIQ real-time PCR detector system based on FAM fluorescence was used for qRT-PCR. The probes used included miR-451 (mmu-miR-451 mouse microRNA-451), cyclin B1 (Mm03053893_gH), *Myc* (Mm00487804_m1), *Inf*g (Mm01168134_m1), *IL4* (Mm00445259_m1), *IL17f* (Mm00521423_m1), *IL10* (Mm01288386_m1), *Sdad1* (Mm00554780_m1), and *Apex1* (Mm01319526_g1). Analysis of change in threshold values ($2^{-\Delta\Delta CT}$) was assessed using an approach previously described by our group [19]. All mRNA values were normalized to at least two housekeeping genes (Tbp [Mm00446971_m1], GAPDH [Mm99999915_g1], 18s ribosomal RNA [Mm03928990_g1], and tubulin [Mm00446971_m1]);

miRNA values were normalized to U6 small nuclear RNA (U6 snRNA 001973) and/or sno202.

T cell transfection

miR-451 Inhibition Activated T helper cells were transfected with a miR-451 antagomiR locked nucleic acid (LNA, Exiqon) or an LNA scrambled control (Exiqon).

miR-451 overexpression Unstimulated T helper cells were transfected with pre-miR-451 (50 pM; Ambion), and scrambled pre-miR negative control (50 pmol; Ambion).

Cells were transfected via electroporation (Lonza).

RNA sequencing

CD4⁺ T cells were purified from WT and miR-451^{-/-} spleens pre- and post-*P. yoelii* infection, and total RNA was isolated using RNeasy Plus Micro Kit (Qiagen). RNA samples were sequenced on an Illumina HiSeq2500 Sequencer using a TruSeq Total-stranded RNAseq library preparation. Reads were mapped to the *Mus musculus* genome (mm10) with SHRiMP2.2.3, and differential expression was determined using cufflinks 2.0.2. *Myc*-regulated genes identified in miR-451^{-/-} CD4⁺ T cells postinfection were displayed using the Google Charts API (Sankey Diagram) [20]. RNA-Seq individual data is in Supplemental data.

Data were analyzed using QIAGEN's Ingenuity® Pathway Analysis (IPA®, QIAGEN Redwood City, www.qiagen.com/ingenuity).

CD4⁺ T cell proliferation

In vivo BrdU Mice were infected with 5×10^5 *P. yoelii* XNL pRBCs. On day 8 postinfection, mice were injected with 1 mg 5-bromo-2'-deoxyuridine (BrdU) (Life Technologies) intraperitoneally. Spleens were collected on day 9 postinfection, cells were stained with anti-BrdU (BU20a; eBioscience), and BrdU incorporation was measured by flow cytometry.

In vitro BrdU CD4⁺ T cells were isolated from spleens, and 25 μM BrdU was added 24 h prior to cell analysis on day 3, 5, and 7 poststimulation. Cells were stained with anti-BrdU (BU20a; eBioscience), and BrdU incorporation was measured by flow cytometry.

In vitro pH 3 Intracellular detection of phosphorylated histone 3 (pH 3) in negatively selected splenic CD4⁺ T cells cultured in vitro was performed by first staining the cell surface with anti-mouse anti-CD4 (RM 4–5; eBioscience). Cells were then permeabilized and stained with anti-human/mouse phospho-Histone H3 (HTA28; eBioscience) for 30 min at

4 °C in the dark. Cells were washed and fluorescence was detected using flow cytometry.

Western blotting

CD4⁺ T cells were isolated from the spleens of mice, and cell lysates were loaded and run on 4–15% Mini-PROTEAN TGX Precast gels (Bio-Rad). Proteins were then transferred onto nitrocellulose membranes using a Trans-Blot SD semidry electrophoresis transfer system. Membranes were immunoblotted using mouse polyclonal antibodies against GAPDH (FL-335), *c-Myc* (9402; Cell Signaling), or monoclonal antibody to cyclin B1 (GNS1). Horseradish peroxidase-conjugated anti-rabbit and anti-mouse (for cyclin B1 detection only) (Sigma-Aldrich) were used along with chemiluminescence to detect protein expression via X-ray film. Protein expression was quantified using ImageJ software.

Statistical analysis

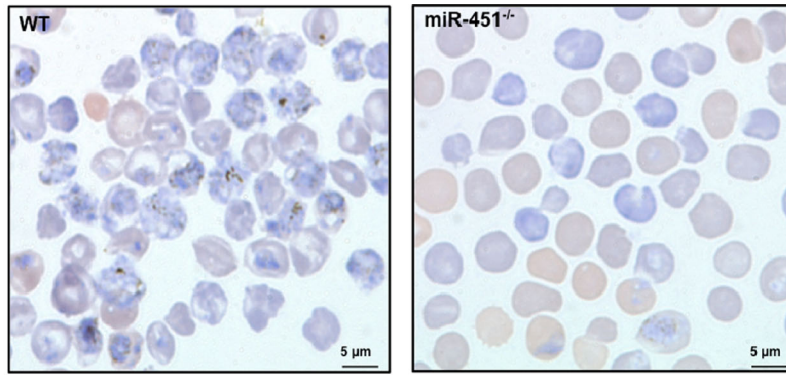
GraphPad Prism software and R version 3.1.0 were used for statistical analysis. For studies that involve the comparison of two groups, unpaired Student's *t* tests were used to determine statistical significance unless otherwise noted. For comparison of means for groups of three or more, two-way repeated measures ANOVA with a Tukey posttest was used.

Results

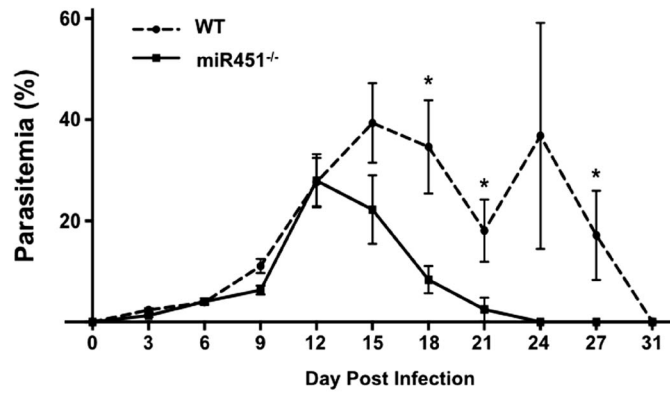
miR-451 negatively regulates parasite clearance during malaria infection

In vitro studies have indicated that miR-451 limits *Plasmodium* parasite growth [7]. To determine whether miR-451 has a similar in vivo function, WT and miR-451^{-/-} mice were infected with blood stage *Plasmodium yoelii* XNL (*P. yoelii* XNL, nonlethal malaria infection model). *P. yoelii* XNL is a self-limiting infection and induces host immune responses to clear the infection [21]. Parasitemia was determined by blood smear on multiple days postinfection. MiR-451^{-/-} mice cleared *P. yoelii* XNL significantly more rapidly than did WT mice (Fig. 1a, b). To determine whether the accelerated miR-451^{-/-} parasite clearance was hematopoietic cell dependent, WT mice were lethally irradiated, bone marrow reconstituted with either WT or miR-451^{-/-} bone marrow, and infected with *P. yoelii* XNL. WT mice reconstituted with miR-451^{-/-} bone marrow cleared the infection at a much faster rate than did mice reconstituted with WT bone marrow (Fig. 1c, d). These data demonstrate that in contrast to in vitro studies, miR-451 does not limit *P. yoelii* in vivo and that enhanced parasite clearance in miR-451^{-/-} mice is driven by a hematopoietic derived cell response to infection.

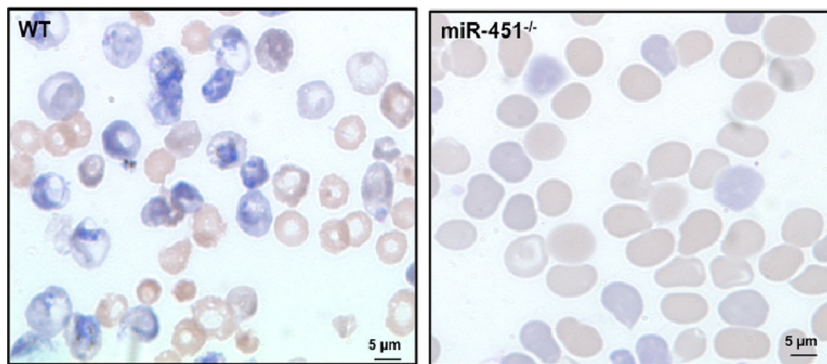
A



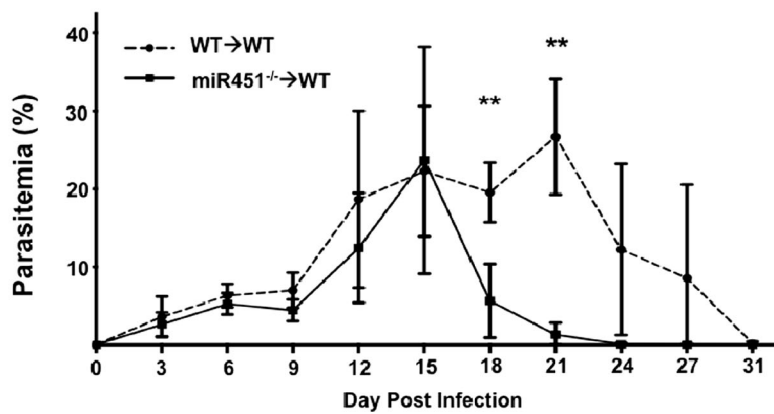
B



C



D



◀ **Fig. 1** miR-451^{-/-} mice have accelerated *P. yoelii* XNL clearance. **a** WT and miR-451^{-/-} mice were infected and parasitemia assessed by Giemsa stained blood smears. Representative smears ($\times 100$, day 21 postinfection). **b** Parasitemia quantification (mean \pm SEM, $N = 5$, $*P < 0.05$, two-way ANOVA with Tukey posttest). Representative of two separate experiments with similar results. **c** Hematopoietic cells mediate miR-451^{-/-} protective effects. WT mice were lethally irradiated and marrow reconstituted with WT or miR-451^{-/-} bone marrow. Mice were infected with *P. yoelii* XNL and parasitemia assessed (representative smear, $\times 100$, day 21 postinfection). **d** Parasitemia quantification (mean \pm SEM, $N = 5$, $**P < 0.01$, two-way ANOVA with Tukey posttest). Representative of two separate experiments with similar results

miR-451^{-/-} mice have increased immune responses to infection

To characterize hematopoietic responses to *P. yoelii* in WT and miR-451^{-/-} mice, complete blood counts (CBC) were performed over the course of infection. Total lymphocyte counts pre-infection were similar between WT and miR-451^{-/-} mice, but total lymphocytes postinfection was increased in miR-451^{-/-} mice, peaking at about postinfection day 9 (Supplemental Table 1). We then determined the changes in specific lymphocyte populations. Innate immune cells were similar between WT and miR-451^{-/-} mice both pre- and postinfection, but postinfection neutrophils were somewhat increased in miR-451^{-/-} mice (Supplemental Table 1). To characterize acquired immune cells, WT and miR-451^{-/-} spleens were harvested pre-infection and on day 9 postinfection, a time point with peak lymphocyte numbers and before the parasitemia diverged between the two groups of mice. There was no difference in B cell numbers either pre- or postinfection (Fig. 2a). WT and miR-451^{-/-} mice had a similar fold change in CD4⁺ and CD8⁺ T cell numbers from pre- to postinfection, but the total numbers of each T cell type were greatly increased in miR-451^{-/-} mice, particularly postinfection (Fig. 2b, c).

CD4⁺ T cells express miR-451 (Supplemental Fig S2) [10, 11] and CD4⁺ T cells are critical in driving *P. yoelii* XNL clearance [13]. To determine whether CD4⁺ cells mediate the protective miR-451^{-/-} phenotype, we treated WT and miR-451^{-/-} mice with either CD4⁺ or CD8⁺ T cell depleting antibody or control IgG (Supplemental Figs. S3–S5), infected the mice, and measured the parasite burden. CD4⁺-depleted WT and miR-451^{-/-} mice had similar parasite burdens (Fig. 2d). Because the protective phenotype was lost when CD4⁺ cells were depleted, it suggested that CD4⁺ T cells have a central role in increased miR-451^{-/-} blood stage parasite clearance. In contrast, when CD8⁺ T cells were depleted, the early parasite burden was increased in miR-451^{-/-} mice, but by day 15 postinfection, CD8⁺-depleted miR-451^{-/-} mice still had significantly improved parasite clearance compared to WT mice (Fig. 2e). These data indicate that the miR-451^{-/-} protective phenotype is at least in part CD4⁺ T cell dependent.

We therefore further characterized miR-451^{-/-} and WT CD4⁺ T cell subsets both pre- and postinfection. MiR-451^{-/-} mice had significantly increased Th1 cells and Th2 pre-infection (Th17 and T reg cells were also increased, but not significantly, Fig. 2f). Postinfection, the total number of Th1, Th17, and T regs was significantly increased in miR-451^{-/-} mice compared to WT mice (Fig. 2g). This was further represented by the fold change in cell numbers from pre- to postinfection (WT vs KO, \pm SEM; Th1 17 ± 3.6 vs 58 ± 15 , Th17 31 ± 8.6 vs 73 ± 14.6 , T reg 12 ± 1.8 vs 53 ± 16.5). Similar results were found in WT mice bone marrow reconstituted with WT and miR-451^{-/-} bone marrow (Fig. 2h). These data demonstrate that miR-451 limits CD4⁺ proliferative responses to *P. yoelii* XNL.

miR-451 negatively regulates CD4⁺ T cell proliferation

We next determined whether increased miR-451^{-/-} CD4⁺ T cell numbers is due to increased cell activation, survival, or proliferation. To compare activation responses, WT and miR-451^{-/-} CD4⁺ T cells were isolated and stimulated with anti-CD3/CD28 antibodies for 48 h and CD25 and CD69 positive cells quantified by flow cytometry. There was not a significant difference in WT and miR-451^{-/-} CD4⁺ T cell activation (Fig. 3a). To compare T cell proliferation, isolated CD4⁺ T cells were stimulated and T cell proliferation measured by total cell count and quantification of phosphorylated histone (pH 3)-positive cells. There was a significant increase in miR-451^{-/-} CD4⁺ T cell numbers (Fig. 3b) and pH 3-positive cells beginning about day 5 poststimulation (Fig. 3c). Stimulated WT and miR-451^{-/-} CD4⁺ T cells were also stained with 7-amino-actinomycin D (7AAD) to quantify cell death. There was no significant difference in cell death between WT and miR-451^{-/-} CD4⁺ T cells (Supplemental Fig. S6). Together, these studies suggest that miR-451^{-/-} CD4⁺ cells have increased proliferation, but no change in activation or survival. They demonstrate a direct effect of miR-451 on CD4⁺ T cell proliferation, WT CD4⁺ T cells were transfected with scramble control or pre-miR-451 to increase miR-451 expression, and cells were activated to stimulate cell proliferation. Additional miR-451 decreased T cell proliferation compared to control transfected T cells (Fig. 3d).

A lack of miR-451 also increased CD4⁺ T cell proliferation in vivo. WT and miR-451^{-/-} mice were infected with *P. yoelii* XNL and proliferation determined on day 9 postinfection by BRDU uptake. MiR-451^{-/-} CD4⁺ T cells had increased cell proliferation as indicated by the total number of BRDU⁺ CD4⁺ cells (Fig. 4a). As a further reflection of an increased proliferative state, we determined CD4⁺ T cell cytokine expression by qRT-PCR on cells isolated from WT and miR-451^{-/-} mice on day 9 postinfection. The expression of *Ifng*, *Il4*, *Il10*, and *Il17* was all increased in miR-451^{-/-} T cells (Fig. 4b–e, *Tbp* and *Rna18s5* for expression normalization).

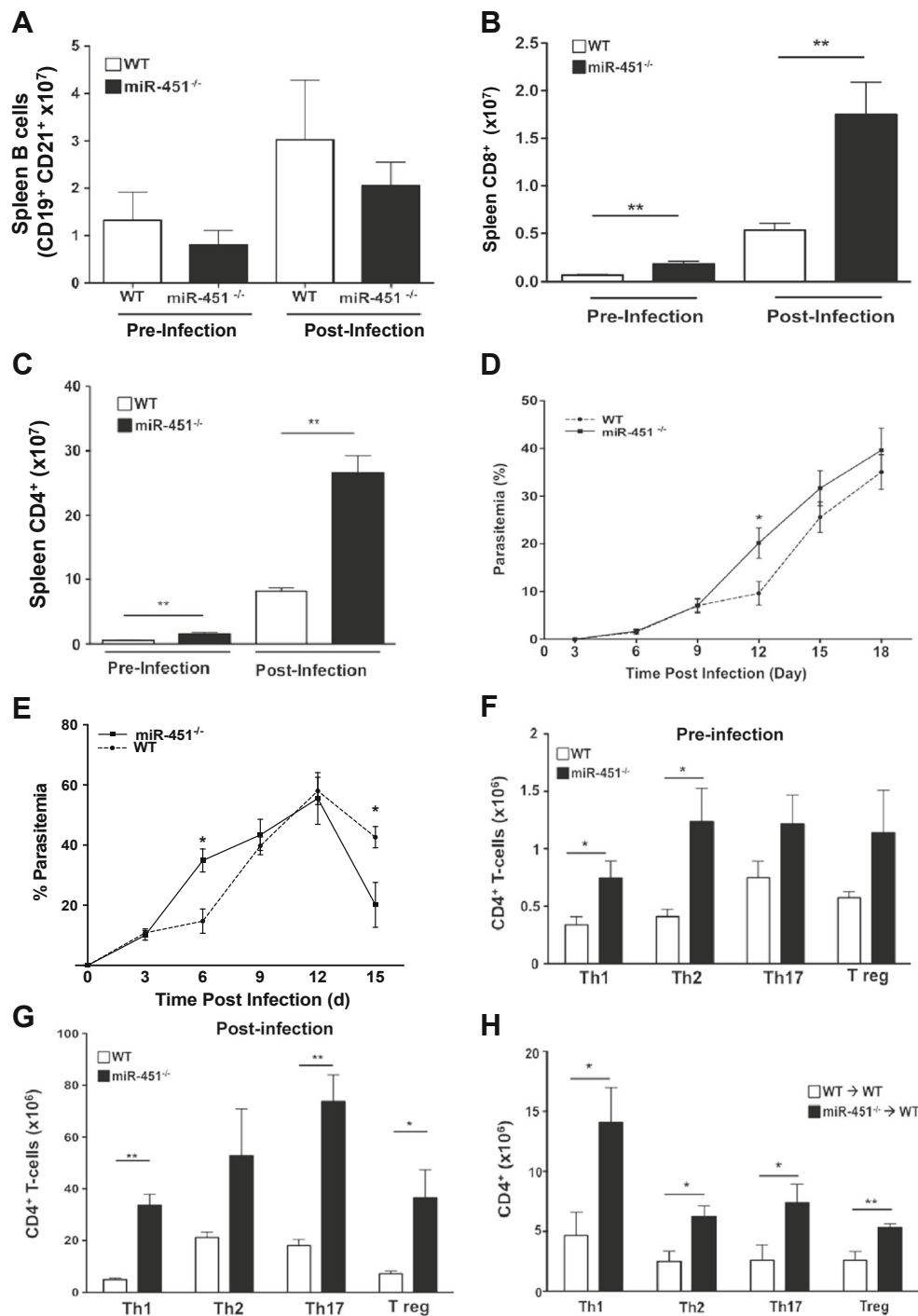
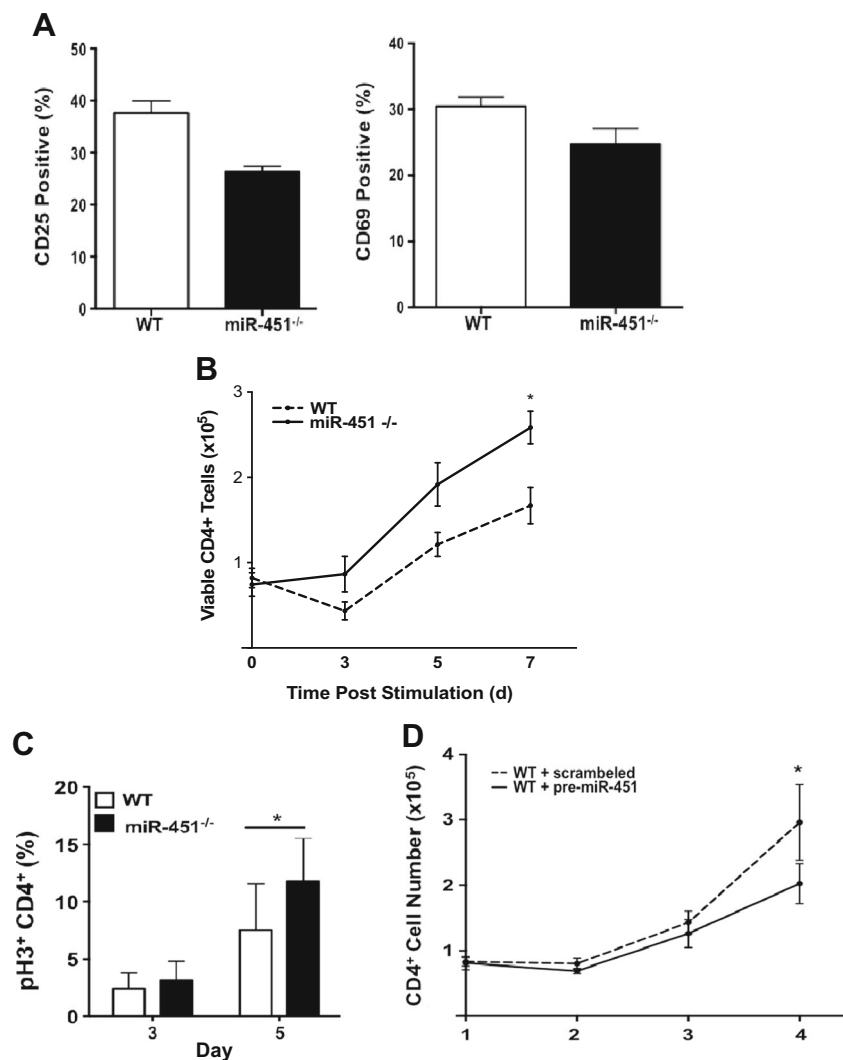


Fig. 2 miR-451^{-/-} mice have increased CD4⁺ T cell responses to infection. Splens were isolated from WT and miR-451^{-/-} mice either pre- or day 9 postinfection. The numbers of **a** B cells, **b** CD8⁺, and **c** CD4⁺ T cells were quantified by flow cytometry. MiR-451^{-/-} mice had increased CD8⁺ and CD4⁺ T cells compared to WT mice (mean ± S.E.M., *N* = 4–5, **P* < 0.01). **d–e** Accelerated parasite clearance in miR-451^{-/-} mice is in part CD4⁺ T cell dependent. Infected WT and miR-451^{-/-} mice were treated with **d** CD4⁺ depleting antibody or **e** CD8⁺ depleting antibody. Parasitemia was determined over time (mean ± S.E.M., *N* = 4–8, **P* < 0.05, two-way ANOVA with Tukey posttest). **f** Baseline T-helper and T reg cells are increased in miR-451^{-/-} mice compared to

WT mice (mean ± S.E.M., *N* = 4–5, **P* < 0.01). **g** CD4⁺ cells are increased in miR-451^{-/-} mice compared to WT mice postinfection. Mice were infected with *P. yoelii* XNL and T helper and T reg numbers determined on day 9 (mean ± S.E.M., *N* = 4–5, **P* < 0.05, ***P* < 0.01). **h** Increased CD4⁺ cell responses are hematopoietic dependent. WT mice were lethally irradiated and bone marrow transplanted with WT or miR-451^{-/-} bone marrow and infected with *P. yoelii* XNL. MiR-451^{-/-} reconstituted mice had increased T helper and T reg responses on day 9 postinfection (mean ± S.E.M., *N* = 4–5, **P* < 0.05, ***P* < 0.01; representative of two separate experiments)

Fig. 3 miR-451 inhibits CD4⁺ T cell proliferation in vitro. **a** WT and miR-451^{-/-} CD4⁺ cells have similar activation. WT and miR-451^{-/-} CD4⁺ cells were stimulated with anti-CD3 and CD28 antibodies and CD25 and CD69 expression determined 48 h later (mean ± S.E.M., *N* = 4). **b**, **c** miR-451^{-/-} CD4⁺ T cells have increased proliferation. CD4⁺ cells from WT and miR-451^{-/-} mice were stimulated. **b** Cell numbers (mean ± S.E.M., *N* = 8, **P* < 0.05, two-way ANOVA with Tukey posttest). **c** pH 3 as a marker of active cell cycle by flow cytometry was determined on multiple days (mean ± S.E.M., *N* = 4, Student's *t* test, **P* < 0.05). **d** Increased miR-451 decreases CD4⁺ T cell proliferation. CD4⁺ cells were treated with miR-451 pre-miRNA or a scrambled control and co-stimulated. Cell numbers were determined (mean ± S.E.M., *N* = 4, **P* < 0.05, paired *t* test)



These in vivo and in vitro data indicate that miR-451 is a negative regulator of cell proliferation and that the protective T helper cell response in miR-451^{-/-} mice is driven by increased CD4⁺ T cell proliferation.

miR-451 targets *Myc* to regulate CD4⁺ T cell proliferation

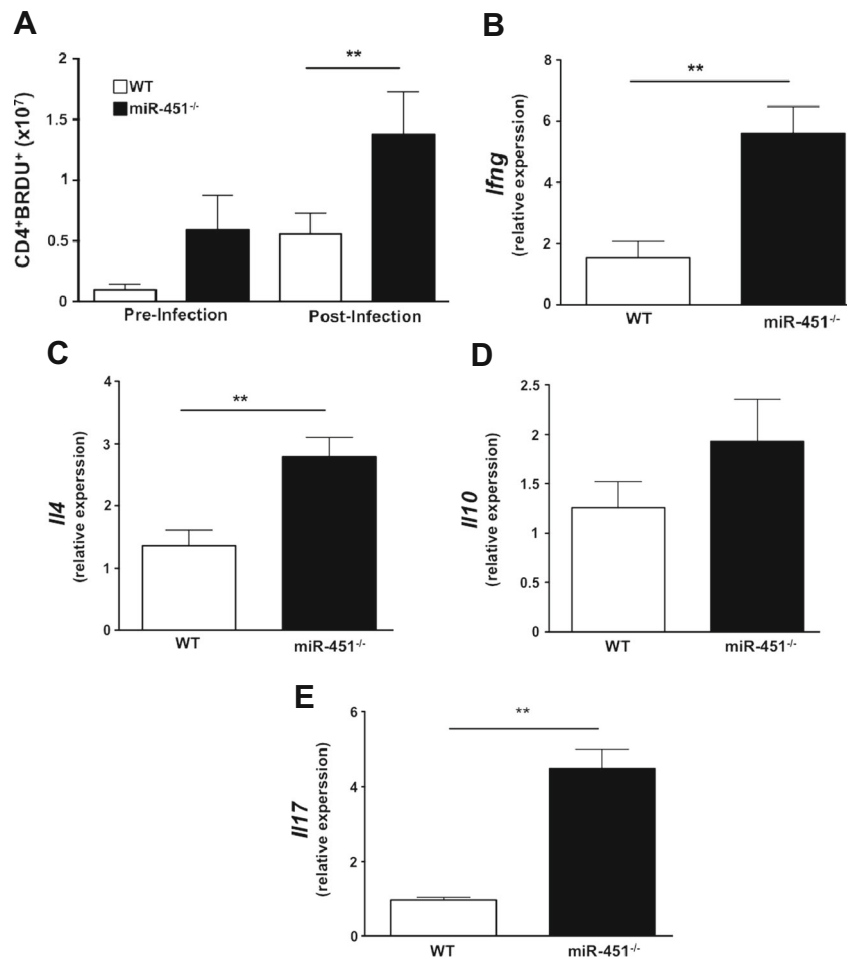
If miR-451 negatively regulates T cell proliferation, miR-451 expression is expected to decrease following T cell activation when cells enter a proliferative state. To demonstrate this, we measured miR-451 expression in WT CD4⁺ T cells pre- and on multiple days post-in vitro activation. There was an approximately 50% reduction in miR-451 expression 48 h post-stimulation and a 70% reduction after 96 h (Fig. 5a). This suggests that miR-451 is downregulated following T cell stimulation.

Myc was identified as a direct miR-451 gene target in a mouse acute lymphoblastic leukemia (T-ALL) model [4].

Myc is a major regulator of cell cycle progression and proliferation of most tissues. To demonstrate that miR-451 regulated *Myc* expression may contribute to increased miR-451^{-/-} CD4⁺ proliferation, we isolated WT and miR-451^{-/-} CD4⁺ T cells and measured *Myc* protein expression before and 9 days after *P. yoelii* XNL infection. There was no difference in *Myc* protein expression between WT and miR-451^{-/-} CD4⁺ T cells at baseline (Fig. 5b). *Myc* was markedly increased postinfection in miR-451^{-/-} CD4⁺ T cells (Fig. 5c). These results were supported by qRT-PCR for *Myc* (Fig. 5d).

To further demonstrate that *Myc* is a potential mediator of increased miR-451^{-/-} CD4⁺ T cell proliferation, we stimulated WT and miR-451^{-/-} CD4⁺ T cells in the presence of a small molecule inhibitor that directly targets *Myc* (10058-F4) [22]. *Myc* inhibitor treatment resulted in WT and miR-451^{-/-} cells having very similar T cell proliferation (Fig. 5e). These results suggest that miR-451 suppression of *Myc*-regulated genes has a direct role in T cell proliferation.

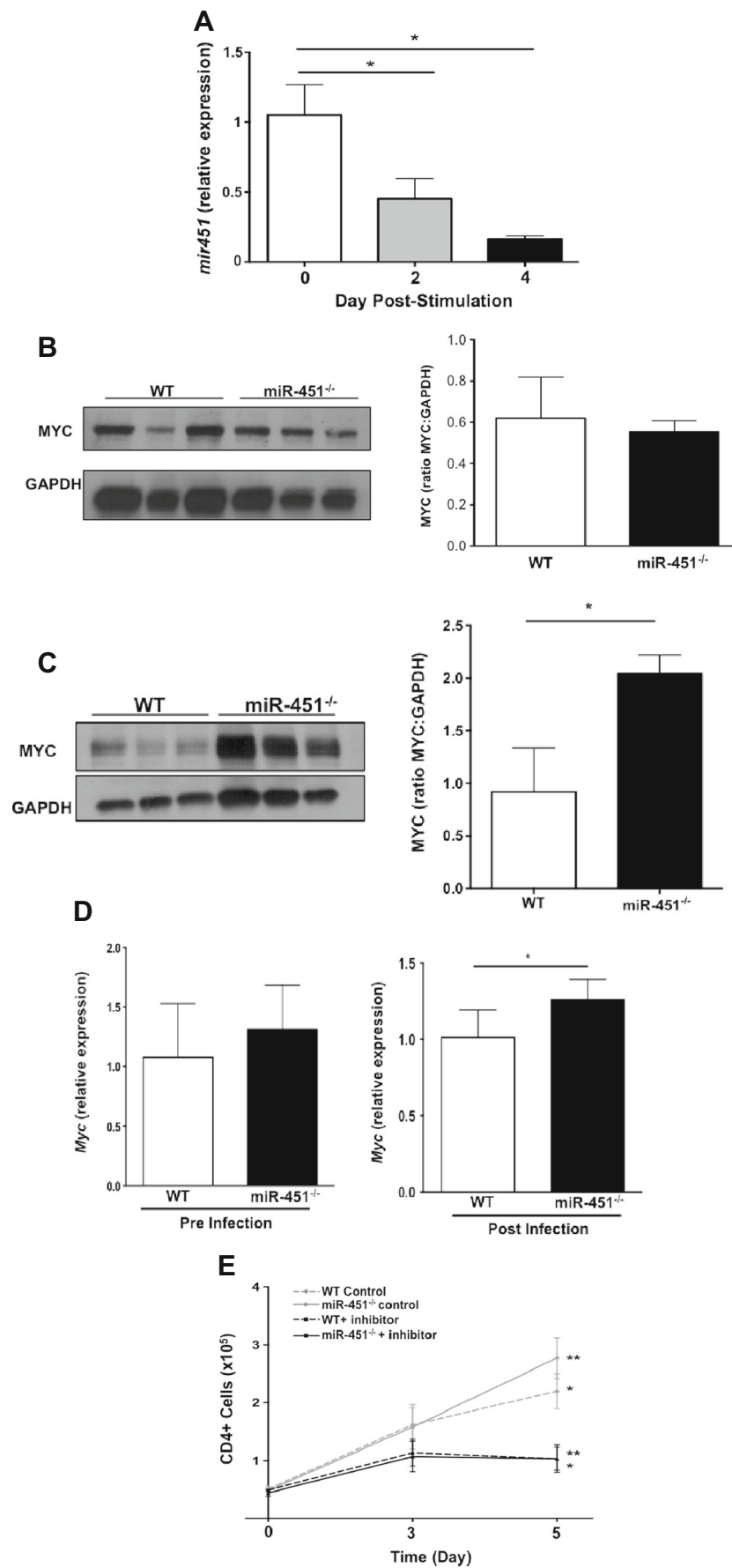
Fig. 4 **a** Mice lacking miR-451 have more in vivo CD4⁺ T cell proliferation both pre- and postinfection as determined by the number of BRDU⁺ CD4⁺ cells (mean ± S.E.M., *N* = 4–5 pre and *N* = 8 postinfection, ***P* < 0.01, representative of two independent experiments). **b–e** miR-451^{-/-} T cells have increased cytokines postinfection. mRNA was isolated from WT and miR-451^{-/-} T cells on day 9 postinfection and qRT-PCR performed for *Ifng*, *Il4*, *Il10*, and *Il17*. *Ifng*, *Il4*, and *Il17*, but not *Il10*, were significantly increased in T cells from miR-451^{-/-} mice (mean ± S.E.M., *N* = 3–4, ***P* < 0.01, relative to *Tbs* and *Rna18s5*)



To identify gene expression changes in miR-451^{-/-} CD4⁺ T cells, we conducted an Illumina TruSeq Total stranded RNA-seq screen on WT and miR-451^{-/-} CD4⁺ T cells isolated both before and on days 6 and 9 post-*P. yoelii* XNL infection (data in Supplemental Excel Table). Pre-infection there were only 82 differentially expressed genes between WT and miR-451^{-/-} T cells (not shown). Postinfection D9, there were over 5000 differentially expressed genes, 4474 of which were up-regulated in miR-451^{-/-} compared to WT CD4⁺ T cells (Fig. 6a). Pathway analysis indicated that a large number of the altered genes were regulators of cell growth and proliferation (Table 1). From these data, we identified Myc-regulated genes increased in miR-451^{-/-} T cells that are involved in cell growth and proliferation [23–26] (confirmed by the gene ontology reference, Panther Classification System) (Fig. 6a, red squares). Our survey identified at least 31 directly Myc-regulated genes involved in cell proliferation that were increased miR-451^{-/-} CD4⁺ cells (Fig. 6b). Among these genes were *Ccnb1*, *Sdad1*, and *Apex1* [25] that we confirmed using qRT-PCR (Fig. 6c–e). To further confirm the effects of miR-451 on Myc-regulated gene expression pathways, we applied Ingenuity Pathway Analysis (IPA). The predicted functional pathways for Myc-regulated genes that were increased in

miR-451^{-/-} CD4⁺ T cells included increased cell proliferation (Fig. 6f) and limiting of cell death (Fig. 6g). These data support a central role for miR-451 in regulating CD4⁺ proliferative responses.

Fig. 5 miR-451 regulates CD4⁺ Myc expression. **a** miR-451 expression is decreased in activated T cells. CD4⁺ T cells were stimulated with anti-CD3 and CD28 antibody and miR-451 expression determined on multiple days (mean ± S.E.M., *N* = 4, **P* < 0.05). **b** WT and miR-451^{-/-} CD4⁺ T cells have similar basal Myc protein expression. CD4⁺ cell lysates were prepared from control WT and miR-451^{-/-} mice and immunoblotted for Myc. Myc was quantified as relative ratio to GAPDH (mean ± S.E.M., *N* = 3). **c** miR-451^{-/-} CD4⁺ T cells have increased postinfection Myc protein expression compared to WT. CD4⁺ T cell lysates were prepared from WT and miR-451^{-/-} mice on day 9 postinfection, immunoblotted for Myc and quantified relative to GAPDH (mean ± S.E.M., *N* = 3; **P* < 0.05). **d** qRT-PCR analysis of *Myc* expression in WT and miR-451^{-/-} CD4⁺ T cells pre- and postmalaria infection (*N* = 4–5, paired *t* test, **P* < 0.05). **e** Myc mediates increased miR-451^{-/-} cell proliferation. CD4⁺ T cells from WT and miR-451^{-/-} mice were isolated, stimulated, and treated with a Myc inhibitor. WT and miR-451^{-/-} CD4⁺ T cells had similar cell proliferation in the presence of Myc inhibitor (mean ± S.E.M., *N* = 3; two-way ANOVA with Tukey posttest; **P* < 0.05, WT control versus WT plus inhibitor; ***P* < 0.05, miR-451^{-/-} control versus miR-451^{-/-} plus inhibitor)



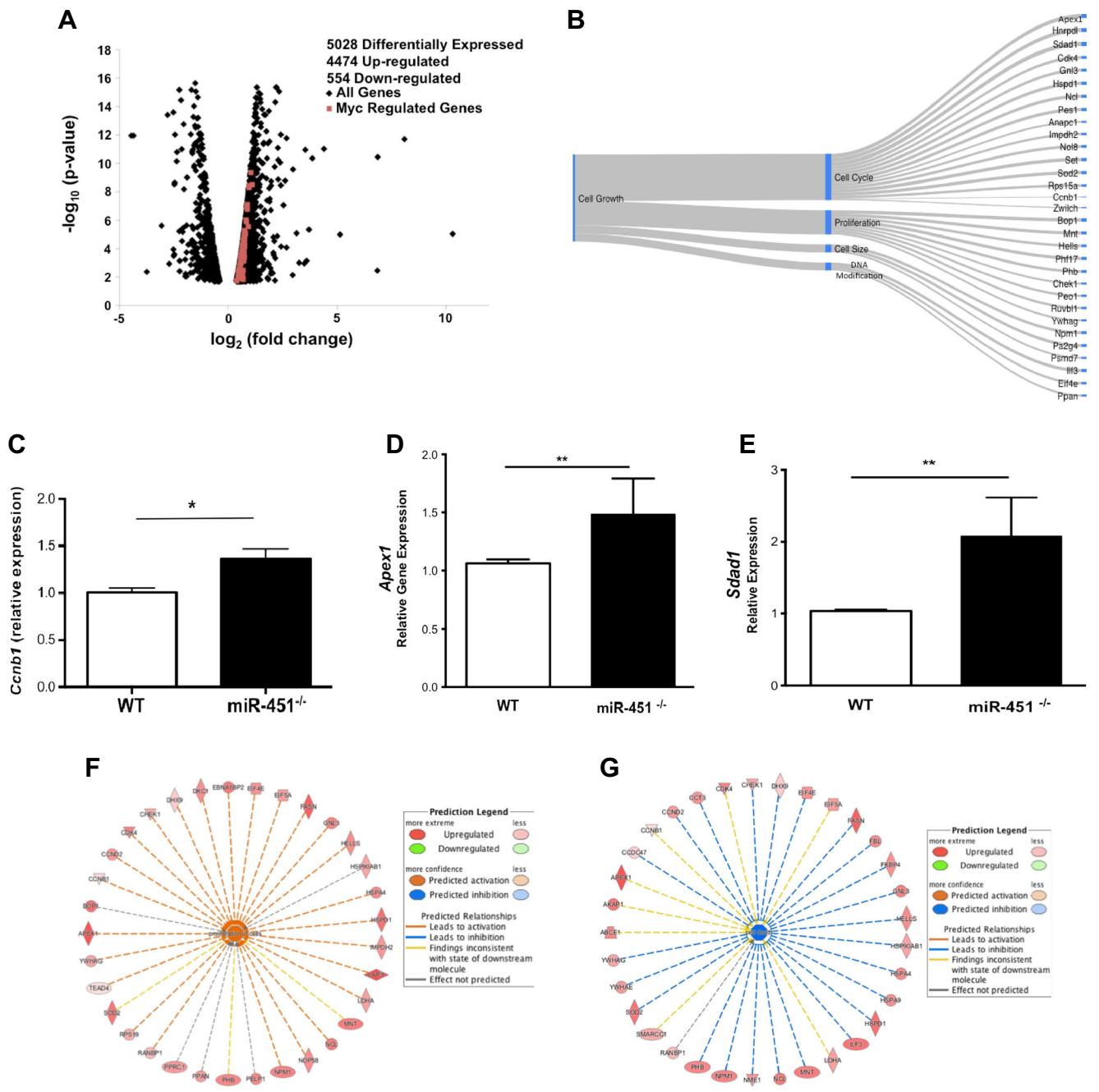


Fig. 6 Expression of Myc target genes is increased in miR-451^{-/-} mice postinfection. CD4⁺ T cells were isolated from WT and miR-451^{-/-} mice on day 9 postinfection and RNA-seq performed. MiR-451^{-/-} versus WT gene expression was compared. **a** Volcano plot (*N* = 2), Myc-regulated genes highlighted. **b** Myc-regulated cell growth-related genes are upregulated in miR-451^{-/-} CD4⁺ T cells post-*P. yoelii* XNL infection.

Google Sankey Chart. **c–e** Myc-regulated gene expression validation by qRT-PCR. **e** *Ccnb1*. **f** *Apex1*. **g** *Sdad1* (*N* = 6, **P* < 0.05, ***P* < 0.01). **f** Predicted effect of Myc-regulated genes with increased expression in miR-451^{-/-} mice. Twenty-five of the 33 genes lead to cell proliferation. **g** Effect of Myc-regulated genes increased in miR-451^{-/-} mice on cell death

Discussion

Our data demonstrated that miR-451 is a regulator of the host immune responses to *Plasmodium* infection. In particular, miR-451 may in part limit CD4⁺ T cell proliferation by regulating *Myc* expression, although a large number of genes are altered postinfection in miR-451^{-/-} CD4⁺ T cells. Mice

lacking miR-451 had a more rapid *P. yoelii* XNL clearance. The increase in parasite clearance was diminished when CD4⁺ cells were antibody depleted indicating that CD4⁺ T cells play a significant role in the miR-451^{-/-} protective phenotype. Other cell types were also increased postinfection in the knockout mice, including neutrophils and CD8⁺ cells, which may be a direct result of a lack of miR-451, or an indirect

Table 1 Functional classification of genes significantly increased in postinfection miR-451^{-/-} CD4⁺ cells compared to WT CD4⁺ cells

Category term	Gene count	P value	Benjamini
Phosphoprotein	1984	7.90E-69	1.60E-66
Nucleus	1231	2.20E-42	2.60E-40
Alternative splicing	1157	1.70E-04	1.60E-03
Acetylation	1081	1.60E-147	9.30E-145
Cytoplasm	975	2.20E-31	1.60E-29
Ion binding	962	1.30E-02	2.40E-01
Nucleotide binding	733	2.00E-34	1.70E-31
Mitochondrion	617	1.80E-92	1.10E-89
Regulation of transcription	560	2.40E-02	3.60E-01
Organelle lumen	544	1.10E-85	2.40E-83
Hydrolase	481	2.40E-14	7.30E-13
Transferase	461	3.30E-17	1.20E-15
Transport	450	2.70E-06	3.80E-05
Protein localization	304	1.80E-26	1.20E-23
Endoplasmic reticulum	300	4.00E-19	1.40E-17
RNA binding	298	2.10E-35	3.50E-32
Proteolysis	292	1.50E-04	6.90E-03
Cellular catabolic process	244	8.10E-21	2.80E-18
Envelope	244	1.30E-31	7.00E-30
Ribonucleoprotein complex	241	2.20E-44	1.70E-42
RNA processing	237	7.00E-45	2.90E-41
Oxidation reduction	225	1.40E-09	1.90E-07
Golgi apparatus	221	2.70E-09	6.10E-08
Kinase	198	6.10E-03	3.80E-02
Nucleolus	194	1.20E-51	1.30E-49
Oxidoreductase	186	1.50E-06	2.20E-05
Cell cycle	179	5.20E-04	2.00E-02
Death	178	1.30E-08	1.40E-06
Ubl conjugation pathway	178	1.20E-10	2.60E-09
Programmed cell death	166	6.70E-09	7.80E-07
Homeostatic process	163	7.70E-03	1.70E-01
Translation	158	2.10E-24	9.90E-22
Vesicle	146	2.70E-03	2.50E-02
Cellular response to stress	144	2.40E-08	2.50E-06
Ligase	122	8.20E-12	2.20E-10
Chromosome	108	6.00E-03	4.80E-02
Ribosome	103	2.20E-20	8.40E-19
Lipid biosynthetic process	102	2.60E-06	2.00E-04
Protein dimerization activity	101	4.10E-03	1.10E-01
Chromatin modification	86	7.60E-06	5.20E-04
Immune system development	83	4.50E-02	5.00E-01
Protein biosynthesis	82	2.20E-18	1.30E-16
Cell division	78	6.70E-02	6.10E-01
Hemopoiesis	72	4.10E-02	4.80E-01
Regulation of growth	72	6.10E-02	5.80E-01

result of increased T-helper cell responses. Malaria pathogenesis is driven by many parts of the immune response, and miR-451 may have a potentially broad immune regulatory role in other cell types as well, either directly or indirectly. This will require more cell by cell analysis.

Our mutant mouse data are in contrast to in vitro studies indicating that increased miR-451 in human sickle cell disease RBCs may contribute to limiting *Plasmodium* growth [27]. The different effects for miR-451 on *Plasmodium* growth in vitro and in vivo may reflect differences between model systems (in vitro vs in vivo models) or the role of individual cell types in isolation versus whole organism systems. This may also indicate that miR-451 has different effects depending on whether its expression is increased or decreased. Our studies show that decreased miR-451 leads to protective immune defects. However, over-expression of miR-451 may not affect the immune response, but rather have a direct effect on parasite growth. These studies clearly indicate that caution is needed when considering the in vivo implications of in vitro miRNA studies, as a miRNA may influence the in vivo responses of many cells and organ systems.

The miR-451^{-/-} protective phenotype is largely CD4⁺ T cell dependent, although it may not be a direct CD4⁺ T cell effect on infected RBCs. The primary function of T helper cells is to direct the activity of other immune cells. We have not yet elucidated the cell type or types that clear infected RBCs in miR-451^{-/-} mice, but because all classes of T helper cells are increased in infected miR-451^{-/-} mice, it is likely that many cell types mediate the accelerated clearance in a manner dependent on CD4⁺ cells. MiR-451^{-/-} mice had more CD8⁺ T cells postinfection, but our cell depletion studies indicated that a role for CD8⁺ cells in parasite clearance was minimal compared to CD4⁺ T cells. Increased CD8⁺ numbers may indicate that miR-451 also has a direct role in regulating CD8⁺ cell proliferation, or increased CD8⁺ cells is an indirect effect of the increased CD4⁺ response. For example, IFN- γ can directly increase CD8⁺ cells during viral infection [28]. A reduction in miR-451 expression also promotes neutrophil chemotaxis [9] and may contribute to the increased postinfection neutrophil count noted in the KO mice. Increased neutrophils may also be an indirect effect of the T helper cell responses, particularly secondary to the increase in Th17 cells.

In this nonlethal malaria model, a lack of miR-451 is protective by driving increased T cell proliferation. In other disease models, such as transplant rejection, the presence of miR-451 may be protective by limiting T cell responses. A number of studies have demonstrated that CD4⁺ T cells are critical in blood stage malaria clearance in both humans [29] and mice [13, 30]. Our study indicates that miR-451 regulation of *Myc* expression in CD4⁺ T cells impacts host immune responses. These data are consistent with a previous study demonstrating that miR-451 regulates *Myc* expression in a mouse model of T-ALL. However, a functional role of miR-451 in the context

of host immune responses has not been described. Our RNA-Seq data revealed over 5000 differentially expressed genes in miR-451^{-/-} CD4⁺ T cells compared to WT CD4⁺ T cell gene expression postinfection. Many *Myc* target genes that promote cell proliferation were upregulated in miR-451^{-/-} CD4⁺ cells suggesting that miR-451 regulation of *Myc* expression is a key regulator of activated T cell proliferation. Given the large number of genes significantly increased postinfection, *Myc* is unlikely to be the only gene involved in the miR-451^{-/-} T cell phenotype. It is likely that miR-451 directly or indirectly regulates multiple gene pathways involved in cell proliferation. Further studies are needed to elucidate these other relevant pathways.

MiRNA has important roles in regulating host immune responses. Our study identifies a unique role for miR-451 in CD4⁺ proliferation potentially impacting our understanding of the immune responses in multiple inflammatory and infectious diseases.

Acknowledgements This work is funded by NIH grants to LMC (F31AI108187) and CNM (R01HL124018) and an American Heart Association (13EIA14250023) to CNM. The project was also supported by the following University of Rochester CTSA awards: TL1 RR024135, TL1 TR000096, UL1 RR024160, and UL1 TR000042 from the National Center for Research Resources and the National Center for Advancing Translational Sciences of the National Institutes of Health.

The authors would like to thank Dr. Eric Olson for the miR-451^{-/-} mice. The authors have no financial conflicts.

References

- O'Connell RM, Rao DS, Chaudhuri AA, Baltimore D. Physiological and pathological roles for microRNAs in the immune system. *Nat Rev Immunol*. 2010;10(2):111–22.
- Rossi RL, Rossetti G, Wenandy L, Curti S, Ripamonti A, Bonnal RJP, et al. Distinct microRNA signatures in human lymphocyte subsets and enforcement of the naive state in CD4⁺ T cells by the microRNA miR-125b. *Nat Immunol*. 2011;12(8):796–803. <http://www.nature.com/nj/journal/v12/n8/abs/ni.2057.html> - supplementary-information
- Johnnidis JB, Harris MH, Wheeler RT, Stehling-Sun S, Lam MH, Kirak O, et al. Regulation of progenitor cell proliferation and granulocyte function by microRNA-223. *Nature*. 2008;451(7182):1125–9. http://www.nature.com/nature/journal/v451/n7182/suppinfo/nature06607_S1.html
- Li X, Sanda T, Look AT, Novina CD, von Boehmer H. Repression of tumor suppressor miR-451 is essential for NOTCH1-induced oncogenesis in T-ALL. *J Exp Med*. 2011;208(4):663–75. doi:10.1084/jem.20102384.
- Patrick DM, Zhang CC, Tao Y, Yao H, Qi X, Schwartz RJ, et al. Defective erythroid differentiation in miR-451 mutant mice mediated by 14-3-3 ζ . *Genes Dev*. 2010;24(15):1614–9. doi:10.1101/gad.1942810.
- Yu D, dos Santos CO, Zhao G, Jiang J, Amigo JD, Khandros E, et al. miR-451 protects against erythroid oxidant stress by repressing 14-3-3 ζ . *Genes Dev*. 2010;24(15):1620–33. doi:10.1101/gad.1942110.
- LaMonte G, Philip N, Reardon J, Lacsina Joshua R, Majoros W, Chapman L, et al. Translocation of sickle cell erythrocyte microRNAs into *Plasmodium falciparum* inhibits parasite translation and contributes to malaria resistance. *Cell Host Microbe*. 2012;12(2):187–99. doi:10.1016/j.chom.2012.06.007.
- Li H-P, Zeng X-C, Zhang B, Long J-T, Zhou B, Tan G-S, et al. miR-451 inhibits cell proliferation in human hepatocellular carcinoma through direct suppression of IKK- β . *Carcinogenesis*. 2013;34(11):2443–51. doi:10.1093/carcin/bgt206.
- Murata K, Yoshitomi H, Furu M, Ishikawa M, Shibuya H, Ito H, et al. MicroRNA-451 down-regulates neutrophil chemotaxis via p38 MAPK. *Arthritis & Rheumatology*. 2014;66(3):549–59. doi:10.1002/art.38269.
- Li X, Sanda T, Look AT, Novina CD, von Boehmer H. Repression of tumor suppressor miR-451 is essential for NOTCH1-induced oncogenesis in T-ALL. *J Exp Med*. 2011;208(4):663–75. doi:10.1084/jem.20102384.
- Smigielska-Czepiel K, van den Berg A, Jellema P, van der Lei RJ, Bijzet J, Kluiver J, et al. Comprehensive analysis of miRNA expression in T-cell subsets of rheumatoid arthritis patients reveals defined signatures of naive and memory Tregs. *Genes Immun*. 2014;15(2):115–25. doi:10.1038/gene.2013.69.
- Organization WH. World Malaria Report 2009. December 2014. <http://www.who.int/features/factfiles/malaria/en/>.
- Butler NS, Moebius J, Pewe LL, Traore B, Doumbo OK, Tygrett LT, et al. Therapeutic blockade of PD-L1 and LAG-3 rapidly clears established blood-stage *Plasmodium* infection. *Nat Immunol*. 2012;13(2):188–95. <http://www.nature.com/nj/journal/v13/n2/abs/ni.2180.html> - supplementary-information
- Vinetz JM, Kumar S, Good MF, Fowlkes BJ, Berzofsky JA, Miller LH. Adoptive transfer of CD8⁺ T cells from immune animals does not transfer immunity to blood stage *Plasmodium yoelii* malaria. *J Immunol*. 1990;144(3):1069–74.
- Scanga CA, Mohan VP, Yu K, Joseph H, Tanaka K, Chan J, et al. Depletion of Cd4⁺ T cells causes reactivation of murine persistent tuberculosis despite continued expression of interferon γ and nitric oxide synthase 2. *J Exp Med*. 2000;192(3):347–58. doi:10.1084/jem.192.3.347.
- George TC, Ortaldo JR, Lemieux S, Kumar V, Bennett M. Tolerance and alloreactivity of the Ly49D subset of murine NK cells. *J Immunol*. 1999;163(4):1859–67.
- Fecci PE, Sweeney AE, Grossi PM, Nair SK, Leam CA, Mitchell DA, et al. Systemic anti-CD25 monoclonal antibody administration safely enhances immunity in murine glioma without eliminating regulatory T cells. *Clin Cancer Res*. 2006;12(14):4294–305. doi:10.1158/1078-0432.ccr-06-0053.
- Kruisbeek AM, Shevach E, Thornton AM. Proliferative assays for T cell function. New Jersey: Current Protocols in Immunology. John Wiley & Sons, Inc.; 2001.
- Shi G, Field DJ, Ko KA, Ture S, Srivastava K, Levy S, et al. Platelet factor 4 limits Th17 differentiation and cardiac allograft rejection. *J Clin Invest*. 2014;124(2):543–52. doi:10.1172/JCI11858.
- Google Charts API Homepage. In: <https://developers.google.com/chart/>. 2015. Accessed November 18, 2014.
- Li C, Seixas E, Langhorne J. Rodent malarial: the mouse as a model for understanding immune responses and pathology induced by the erythrocytic stages of the parasite. *Med Microbiol Immunol*. 2001;189(3):115–26. doi:10.1007/s430-001-8017-8.
- Wang H, Hammoudeh DI, Follis AV, Reese BE, Lazo JS, Metallo SJ, et al. Improved low molecular weight Myc-max inhibitors. *Mol Cancer Ther*. 2007;6(9):2399–408. doi:10.1158/1535-7163.mct-07-0005.
- Ji H, Wu G, Zhan X, Nolan A, Koh C, De Marzo A, et al. Cell-type independent MYC target genes reveal a primordial signature involved in biomass accumulation. *PLoS One*. 2011;6(10):e26057. doi:10.1371/journal.pone.0026057.
- Marinkovic D, Marinkovic T, Kokai E, Barth T, Möller P, Wirth T. Identification of novel Myc target genes with a potential role in

- lymphomagenesis. *Nucleic Acids Res.* 2004;32(18):5368–78. doi:10.1093/nar/gkh877.
25. Menssen A, Hermeking H. Characterization of the c-MYC-regulated transcriptome by SAGE: identification and analysis of c-MYC target genes. *Proc Natl Acad Sci.* 2002;99(9):6274–9. doi:10.1073/pnas.082005599.
 26. Zeller K, Jegga A, Aronow B, O'Donnell K, Dang C. An integrated database of genes responsive to the Myc oncogenic transcription factor: identification of direct genomic targets. *Genome Biol.* 2003;4(10):R69.
 27. LaMonte G, Philip N, Reardon J, Lacsina JR, Majoros W, Chapman L, et al. Translocation of sickle cell erythrocyte microRNAs into *Plasmodium falciparum* inhibits parasite translation and contributes to malaria resistance. *Cell Host Microbe.* 2012;12(2):187–99. doi:10.1016/j.chom.2012.06.007.
 28. Whitmire JK, Tan JT, Whitton JL. Interferon-gamma acts directly on CD8+ T cells to increase their abundance during virus infection. *J Exp Med.* 2005;201(7):1053–9. doi:10.1084/jem.20041463.
 29. Pombo DJ, Lawrence G, Hirunpetcharat C, Rzepczyk C, Bryden M, Cloonan N, et al. Immunity to malaria after administration of ultra-low doses of red cells infected with *Plasmodium falciparum*. *Lancet.* 2002;360(9333):610–7. doi:10.1016/S0140-6736(02)09784-2.
 30. Muxel SM, Freitas do Rosário AP, Zago CA, Castillo-Méndez SI, Sardinha LR, Rodríguez-Málaga SM, et al. The spleen CD⁴ T cell response to blood-stage *Plasmodium chabaudi* malaria develops in two phases characterized by different properties. *PLoS One.* 2011;6(7):e22434. doi:10.1371/journal.pone.0022434.